Dissipation in palladium nanomechanical resonator at ultra low temperatures.

Indrajeet

A dissertation submitted for the partial fulfilment of BS-MS dual degree in Science

Indian Institute of Science Education and Research Mohali
April 2014

Certificate of Examination

This is to certify that the dissertation titled "Dissipation in palladium nanomechanical resonator at ultra low temperatures." submitted by Mr.Indrajeet (Reg.No. MS09062) for the partial fulfillment of BS-MS dual degree programme of the Institute, has been examined by the thesis committee duly appointed by the Institute. The committee finds the work done by the candidate satisfactory and recommends that the report be accepted.

Dr.Ananth Venkatesan (Supervisor) Dr.Sudeshna Sinha Dr. Goutam Sheet

Dated: April , 2014

Declaration

The work presented in this dissertation has been carried out by me under the guidance of Dr. Ananth Venkatesan at the Indian Institute of Science Education and Research Mohali.
This work has not been submitted in part or in full for a degree, a diploma, or a fellowship to any other university or institute. Whenever contributions of others are involved, every effort is made to indicate this clearly, with due acknowledgement of collaborative research and discussions. This thesis is a bona fide record of original work done by me and all sources listed within have been detailed in the bibliography.

Indrajeet
(Candidate)
Dated: April , 2014

In my capacity as the supervisor of the candidate's project work, I certify that the above statements by the candidate are true to the best of my knowledge.

Dr. Ananth Venkatesan
(Supervisor)

Acknowledgement

First of all, I would thank my supervisor, Dr. Ananth Venkatesan, for providing me opportunity to work under him. This work is possible due to his encouragement, ideas, guidance and advice.I would like to thank Prof. Dr.D. Weiss from University of Regensburg for allowing Dr. Venkatesan to use their facility ,so that we are able to fabricate our samples.
I would like to thank Shishram Rebari (Ph.D Scholar) and Abhishek (MS student) who were also working on various aspects of this project.I am also thankful my other lab-mates and Dr. Satyendra Prakash Pal for always finding time to provide help and advice.I would also like to thank Inderjeet Singh for the SEM imaging and Avtar Singh for their help.
I am grateful to my parents for their support and encouragement in everything I pursued.

Abstract

Initial results from the study of dissipation in nanomechanical palladium resonator of width around 250 nm, thickness 80 nm and length 5 μm suspended over the underlying silicon substrate are presented. The electromechanical response of the resonator was measured using the magnetomotive method over the temperature range from 1 K to 145 mK. The resonator had a fundamental frequency of about 33.83 MHz at low temperature different .Differential thermal contraction between the palladium beam and the underlying silicon substrate increases the tension which may have caused this high frequency.Two fold increase the quality factor of the resonator was observed between 1 K and 145 mK. The dissipation follows a weak power law dependence on temperature, $T^{0.47}$ from approximately 200 mK to 1 K. The relative shift in frequency shows logarithmic dependence on temperature.

Contents

List of Figures

List of Tables

Chapter 1

Introduction

Miniaturization of electromechanical devices in recent years has led to emergence the nanoelectromechanical systems (NEMS), with even smaller dimensions than its predecessor microelectromechanical systems (MEMS) .The motivation for miniaturization is the ability to detect very small physical quantities like the device with a mass sensitivity resolution of 7 zeptograms(7 x 10^{-21}) , equivalent to 30 xenon atoms (Yang et al. 2006) and Single electron spin detection using Magnetic Resonance Force Microscopy (Rugar et al. 2004) have been accomplished.Another reason is an opportunity to see quantum effects in macroscopic devices(Armour, Blencowe, and Schwab 2002) (Cho 2003)(Knobel and Cleland 2003) (LaHaye et al. 2004). The mechanical motion of nanoscale resonators is expected to approach the quantum regime by decreasing the size of mechanical devices thus increasing their resonant frequency, and cooling them down to mK temperatures ($\hbar\omega \gg k_B T$).
The performance of nanomechanical resonators for the applications mentioned and for studying quantum effects is often limited by dissipation (energy loss) in the device. The dissipation is quantified by a number known as the Q-factor (Q = $1/dissipation$), the higher it is, the smaller the dissipation. Resonators of fundamental frequency of more than 1GHz have been developed but they yielded poor quality factor of about 500 at low temperature(Henry Huang et al. 2003).We need to understand the dissipation mechanisms at low temperatures in order to maximize the potential of NEMS . Few experiments have been done to understand dissipation in metallic(Venkatesan et al. 2009)(Hoehne et al. 2010) and carbon(Sazonova et al. 2004) nanoresonators at low temperatures which explained dissipation using Standard Tunneling Model. Further experiments are required to be able to draw more firm conclusions about the dissipation mechanisms in such structures.

Chapter 2

Theoretical Background

2.1 Resonant systems

A mechanical system having natural frequency f_o starts to oscillate with f driven by periodic force of frequency f. The condition at which this frequency of driving force matches to the natural frequency f_o of the system due to which the amount of energy absorbed and amplitude oscillation is maximum is called resonance. Harmonic oscillator can be considered as one of the simplest example of mechanical resonant system. Resonant frequency and the quality factor Q characterize this phenomenon. The basic features of resonance can be understand through a simple model of simple harmonic oscillator.(French 1971)(Pain 2005)

2.1.1 Harmonic Motion

Consider a mass m attached to a spring that moves along a straight line with coordinate x, under the action of a force F whose magnitude is proportional with x and represented by

$$F = -kx \tag{2.1}$$

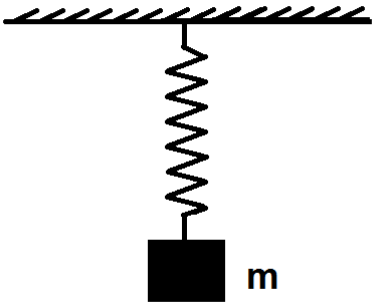

Figure 2.1: A mass m suspended by a spring of spring constant k

where k is the spring constant and negative sign represent that force is in opposite direction to the displacement. The equation of motion can be written as

$$m\ddot{x} + kx = 0 \tag{2.2}$$

whose general solution is given by

$$x = A\cos\sqrt{\frac{k}{m}}t + B\sin\sqrt{\frac{k}{m}}t \tag{2.3}$$

where A and B are any constants.The mass oscillates forever with frequency given by $\omega_o = \sqrt{\frac{k}{m}}$ and constant amplitude about the equilibrium position without any loss in energy.

2.1.2 Damped Harmonic Motion

In real system the oscillation of resonator always dies out with passage of time due to some kind of frictional force. This frictional force is being taken proportional to velocity and it acts in direction opposite to that of the velocity.The equation of motion then becomes

$$m\ddot{x} + \gamma\dot{x} + kx = 0 \tag{2.4}$$

where γ is the proportionality constant. When the coefficient m, γ and k are constant,a solution of form $x = e^{\omega t}$ can always be found, where ω satisfies the characteristic equation

$\omega^2 + 2\gamma\omega + \omega_o^2 = 0$ where $\omega_o^2 = \dfrac{k}{m}$.The solutions are given by(French 1971)

$$\omega_{\pm} = -\frac{\gamma}{2} \pm \sqrt{\frac{\gamma^2}{4} - \omega_o^2} = -\frac{\gamma}{2} \pm \omega_o \sqrt{\frac{\gamma^2}{4\omega_o^2} - 1} \tag{2.5}$$

the general solution of the system is given by(French 1971)

$$x(t) = Ce^{\omega_+ t} + De^{\omega_- t}$$

$$= e^{\frac{-\gamma t}{2}} \left(Ce^{\left(\omega_o \sqrt{\frac{\gamma^2}{4\omega_o^2} - 1}\right) t} + De^{\left(-\omega_o \sqrt{\frac{\gamma^2}{4\omega_o^2} - 1}\right) t} \right) \tag{2.6}$$

The first term describes the damping envelope that bounds the decaying oscillation and the second term (in parentheses) defines the oscillatory part. The system behaves different for following conditions

For $\dfrac{\gamma^2}{4\omega_o^2} - 1 > 0$,the system is over damped.

For $\dfrac{\gamma^2}{4\omega_o^2} - 1 = 0$,the system is critically damped.

For $\dfrac{\gamma^2}{4\omega_o^2} < 1 = 0$,the system is slightly damped and gives oscillatory damped simple harmonic motion.for this case equation 2.6 can be written as

$$x(t) = Ae^{-\frac{\gamma t}{2}} sin(\omega' t + \phi) \tag{2.7}$$

where A and ϕ are constants and $\omega' = \omega_o \sqrt{1 - \dfrac{1}{4Q^2}}$

$Q = \dfrac{\omega_o}{\gamma}$ is called quality factor of the system.

2.1.3 Forced Harmonic Motion

To prevent oscillations from dying out,a periodic force is generally applied to a damped harmonic oscillator. The amplitude of oscillation can be made large by applying force with a frequency close to the natural frequency of the oscillator. The amplitude remains small if the frequency of the applied force is not equal to the natural frequency of the system even if the force is applied repeatedly. Suppose the harmonic oscillator is driven by a periodic

force $F(t) = F_o \cos(\omega t)$. The equation of motion for the system is given by

$$m\ddot{x} + \gamma\dot{x} + kx = F \tag{2.8}$$

The periodic force try to impose its own frequency to the system which wants to oscillates with its fundamental frequency. The solution for this case has two terms. The first term corresponds to the solution of the equation for $m\ddot{x} + \gamma\dot{x} + kx = 0$. For time longer than the damping time, this term can be neglected since the amplitude decays exponentially. The second describes the behavior of the oscillator after the transient term has died. If motion is harmonic of same frequency as of the driving force,the steady state solution is(French 1971)

$$x(t) = \frac{\frac{F}{m}}{\omega_o^2 - \omega^2 + i\frac{\omega\omega_o}{Q}} \tag{2.9}$$

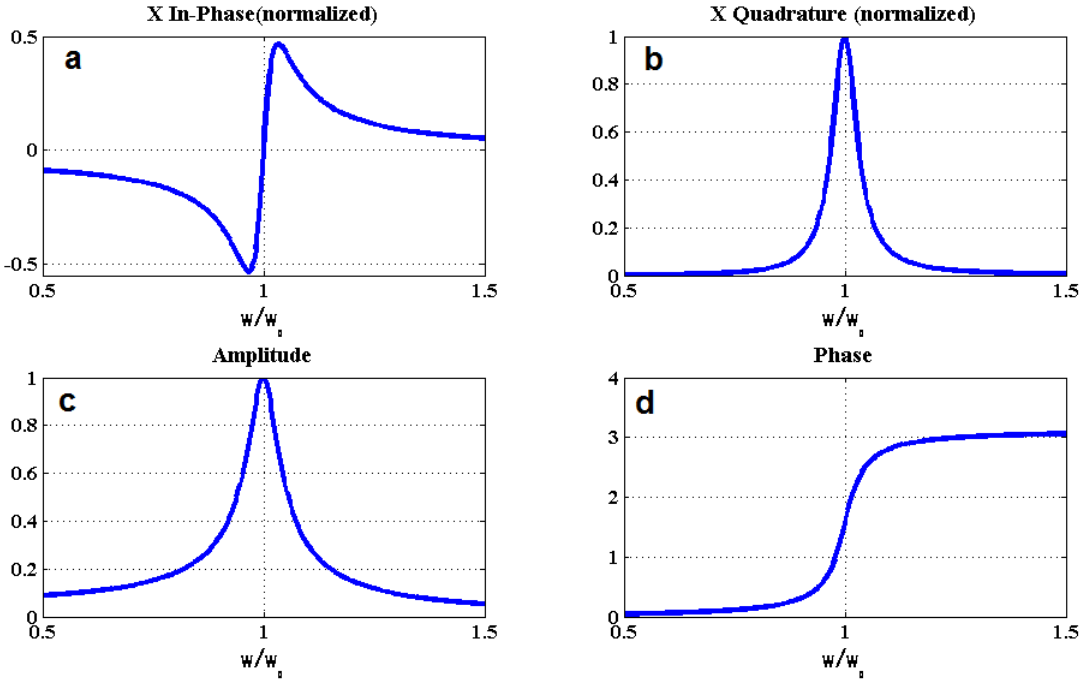

Figure 2.2: (a) In-phase, (b) quadrature (c) absolute amplitude and (d) phase response of a driven damped harmonic oscillator as a function of driving frequency ω.

Real part of x,which is known as 'In-phase' amplitude is

$$Re(x) = \frac{\frac{F}{m}(\omega_o^2 - \omega^2)}{\omega_o^2 - \omega^2 + \frac{\omega_o^2}{Q^2}} \tag{2.10}$$

and imaginary part of x,which is known as 'quadrature amplitude' is

$$Re(x) = \frac{\frac{F}{m}(\frac{\omega\omega_o}{Q})}{\omega_o^2 - \omega^2 + \frac{\omega_o^2}{Q^2}} \tag{2.11}$$

The solution can also be expressed as $x = Ae^{-i\phi}$,where A is the amplitude and ϕ is the phase

$$A(w) = \frac{\frac{F}{m}}{\sqrt{(\omega_o^2 - \omega^2)^2 + (\frac{\omega\omega_o}{Q})^2}} \tag{2.12}$$

$$\phi(\omega) = \arctan \frac{\omega\omega_o}{Q(\omega_o^2 - \omega^2)} \tag{2.13}$$

The amplitude response has the form of a Lorentzian with a peak at ω_o. The quality factor Q is given by $Q = \frac{\omega_o}{\Delta\omega}$ where $\Delta\omega$ is full width at half maximum of the Lorentzian curve fig 2.2.

2.2 Natural Frequency

A doubly-clamped beam is considered with length L,width W and thickness h with coordinate system as shown in the figure 2.3.

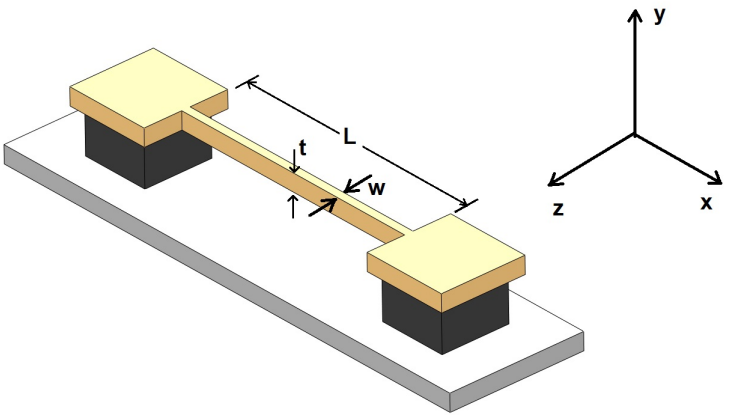

Figure 2.3: A beam of length L , width w and thickness t

For a structure with length is much larger than its cross section area, it is possible to derive a equation for the natural frequencies of oscillations considering linear forces and ignoring any other complicated mechanical effects,the wave equation for the flexural motion of such a beam is given by(Cleland and Roukes 2002)

$$EI\frac{\partial^4 z}{\partial x^4} - T_o\frac{\partial^2 z}{\partial x^2} + \rho A\frac{\partial^2 z}{\partial t^2} = 0 \tag{2.14}$$

where E is the Youngs modulus, $I = \dfrac{Wh^3}{12}$ is the moment of inertia of the beam, T_o is the intrinsic tension in the beam,ρ is the density and A the cross-sectional area .Equation 2.14 is the Euler-Bernoulli Equation with a tension term.The two clamped ends impose the boundary conditions:

$$z(0,t) = z(L,t) = \frac{\partial z}{\partial x}(0,t) = \frac{\partial z}{\partial x}(L,t) = 0 \tag{2.15}$$

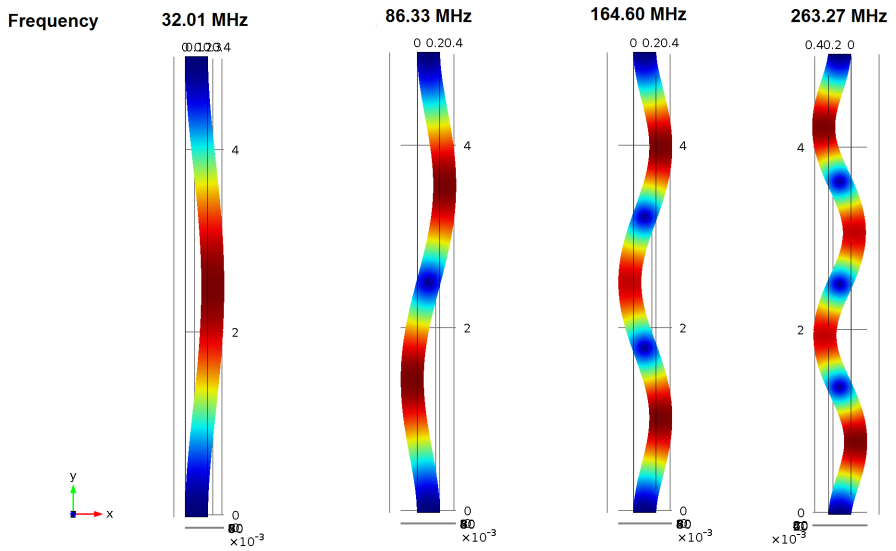

Figure 2.4: First four in-plane flexural resonant mode for studied beam using Comsol

An analytic expression to calculate the mode frequencies is derived in literature:(Bokaian 1990)

$$f_{on} = \frac{\pi}{8}(2n+1)^2 \frac{1}{L^2}\sqrt{\frac{EI}{\rho A}}\sqrt{1+\frac{0.97T_oL^2}{(n+1)^2\pi^2 EI}} \tag{2.16}$$

Figure 2.4 shows the first four in-plane flexural resonant mode for a palladium beam with similar dimension to the measured sample calculated using Comsol. The analytic expression for fundamental mode of a doubly-clamped beam is by (Kozinsky 2007)

$$f_{o1} = \frac{2\pi}{L^2}\sqrt{\frac{EI}{3\rho A}\left(1+\frac{L^2T_o}{4\pi^2 EI}\right)} \tag{2.17}$$

which is similar to equation (2.16) for $n = 1$

2.3 Dissipation

Dissipation (Q^{-1}) is defined as the energy lost per cycle of oscillation (ΔW) as a fraction of the total mechanical energy (W_o) of the resonator. When the drive force stops abruptly dissipation determines the time for which the resonator continues to oscillate.It also determines the transient time of the dynamic system, the time after which the harmonic response of the resonator becomes independent of the initial conditions. The quality factor Q ,i.e. the inverse of the dissipation and the resonant frequency f_o, are the two most important

characteristics of a resonator. Dissipation can be written as

$$Q^{-1} = \frac{\Delta W}{W_o} = \frac{\gamma}{\omega_o} = \frac{\Delta\omega_o}{\omega_o} \tag{2.18}$$

ω_o is the resonance frequency; and γ is the friction, or damping, $\Delta\omega_o$ is the full width at half maximum (FWHM) frequency response. Energy lost through dissipation can be transferred as elastic energy out of the resonator; converted to non-mechanical energy; or lost to the thermal bath as heat.Therefore the total dissipation is written as sum of dissipation caused by different mechanisms.

$$Q^{-1} = Q_1^{-1} + Q_2^{-1} + Q_3^{-1} + ... \tag{2.19}$$

These process are mainly divided in two categories: **Extrinsic Dissipation** includes dissipative mechanisms that are related to engineering constraints and environmental factors like clamping and viscous forces.**Intrinsic Dissipation** considers losses within the material itself, namely thermoelastic dissipation, surface losses , mechanical defects , and quantum dissipation occurring through **two level systems**.

2.3.1 Extrinsic Dissipation

Clamping Loss

From a vibrating resonator, acoustic wave can propagate into the substrate causing the resonator to lose energy. If the acoustic waves have wavelength comparable to the beam length, most of the waves are reflected back and clamping loss is minimum. These losses are expected to be temperature independent.In the reference a approximation for clamping dissipation for a cantilever is by:(Photiadis and Judge 2004)

$$Q_{cl}^{-1} = \frac{wt^3}{3.2l^5} \tag{2.20}$$

where w,t and l are width,thickness and length of the cantilever.

Fluid Friction

Resonators can dissipate energy in gaseous environment due to collision with gas molecules., So the dissipation increases if the surrounding pressure is increased. At very low pressures, where the mean free path of the fluid molecules is much larger than the device dimensions $Q^{-1} \backsim p$(Bhiladvala and Wang 2004) however $Q^{-1} \backsim \sqrt{p}$ when the pressure is

higher.(V.A.Sazonova 2006) A good vacuum can be used to minimize such type of damping.

Dissipation due to measurement setup

Attempts to measure the mechanical motion typically tend to cause some disturbance of the motion, and often lead to additional damping.For example,In the magnetomotive technique used the EMF generated in the device will also give rise to eddy currents that produce another force opposite to the motion of the beam and has an effect of adding more damping to the resonator.

2.3.2 Intrinsic Dissipation

Thermoelastic Effect

Local temperature gradient across the resonator can be induced,when subjected to mechanical vibrations due to the rapid expansion and contraction in the structure . hence heat flows from hot to cold regions. The resonator tries to relax back to equilibrium by coupling to the thermal modes of the surrounding environment which make it a temperature dependent process. The temperature dependence of thermoelastic damping for thin vibrating beams is

$$Q^{-1} = \frac{E\alpha T^2}{C_p} P \tag{2.21}$$

Where E is the Youngs modulus, $\alpha = \frac{1}{L}\frac{\partial L}{\partial T}$ is the thermal expansion coefficient, T is the temperature, C_p the heat capacity at constant pressure and P is a constant which depends on the beam materials thermal diffusivity.(Lifshitz and Roukes 2000)

Surface Effects

With the change in surface-to-volume ratio of resonator, quality factor also changes which suggests that the surface of nanomechanical resonator also plays an important role in dissipation.(Ekinci and Roukes 2005) The presence of oxide or water layer or dangling bonds on the surface of resonator can be the cause of such losses. Methods like annealing or surface passivation can be implemented to minimized these losses.

2.3.3 Two-level systems: Standard Tunneling Model

The standard tunneling model was proposed simultaneously by Phillips (Phillips 1972) and Anderson (Anderson, Halperin, and Varma 1972) to explain the properties of disordered solid at low temperatures.

The STM predicts that the presence of defects in solids, such as dangling bonds, contaminants or dislocations can be the cause of damping due to leads to the existence of anharmonic excitations . A double well potential model can be applied to these defects where,at low temperature an atom or group of atoms can occupy one of two possible energy minima separated by an energy barrier height V as depicted schematically in Figure 2.5.

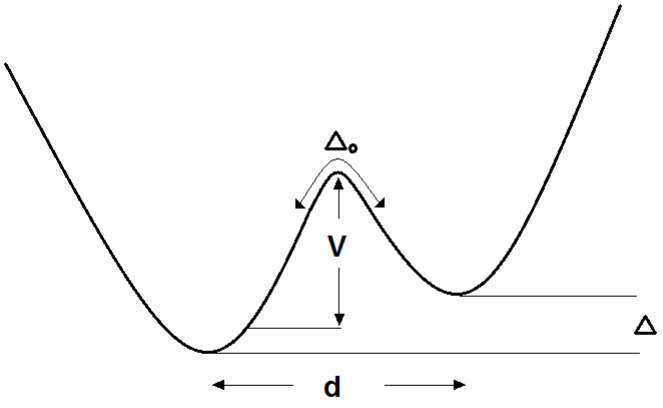

Figure 2.5: The double well potential model for defects in a solid, with barrier height V , width d, asymmetry Δ and tunnelling energy Δ_o.

At low temperatures only the ground states of both wells play a role in the dynamics hence it is defined as a two-level system (**TLS**).The TLS can couple to their environment via strain and electric fields.So initially it absorbs energy from the mechanical motion which modifies the strain field and then releases the energy through interactions with phonons and conduction electrons (in the case of metallic structures) via two processes: resonant and relaxation absorption.when an external acoustic wave excites vibrational mode of the resonator with angular frequency ω the mechanism of dissipation depends on the ratio $\frac{\hbar\omega}{k_B T}$,

where $\hbar\omega$ is the energy of the acoustic wave. If $\frac{\hbar\omega}{k_BT} \geq 1$, then the phonons can be resonantly absorbed by those defects and the TLS will undergo a transition from the ground state into the excited state.In this regime the contribution to the damping is negligible and a measurable temperature dependence for the shift in frequency of the resonator can be observed.

In the regime where $\frac{\hbar\omega}{k_BT} \leq 1$ there can still be dissipation in the vibrating element via anelastic effects due to the phase delay between the stress and imposed strain. The acoustic wave couples to the TLS and changes its thermal equilibrium by modifying Δ or Δ_o. The TLS then tries to relax to a new equilibrium position by absorbing and emitting thermal phonons,which causes dissipation and a shift in the resonant frequency of the resonator.The ratio between the mechanical period and the relaxation time τ of the TLS determines the strength of relaxation damping . Maximum damping occurs when

$$\omega\tau \sim 1 \tag{2.22}$$

i.e the mechanical period of the resonator matches the relaxation time of the TLS. The broad distribution of tunnel splittings, Δ_o, means that there is a broad range of relaxation rates. There exists a well-defined minimum,$\tau_{min}(E)$ at each energy E $\sim K_BT$ for the relaxation mechanisms relevant for TLS in amorphous solids .(Hunklinger and Raychaudhuri 2011) (Phillips 1987) The temperature corrosponding to the condition when $\omega\tau_{min} \sim 1$ is called crossover temperature T^*. Below T^* i.e. $\omega\tau_{min} \gg 1$, , the dissipation is proportional to T^n where n = 3(1) depending on whether the relaxation is through phonons (electrons).
Above T^* i.e. $\omega\tau_{min} \ll 1$, the damping is given by

$$Q^{-1} = \frac{\pi}{2}C \tag{2.23}$$

where $C = \frac{P_o\eta^2}{\rho v^2}$ is a constant which depends on the density of states of the TLS in the structure . The parameter η is the change in the TLS asymmetry per unit strain and v is the speed of sound.

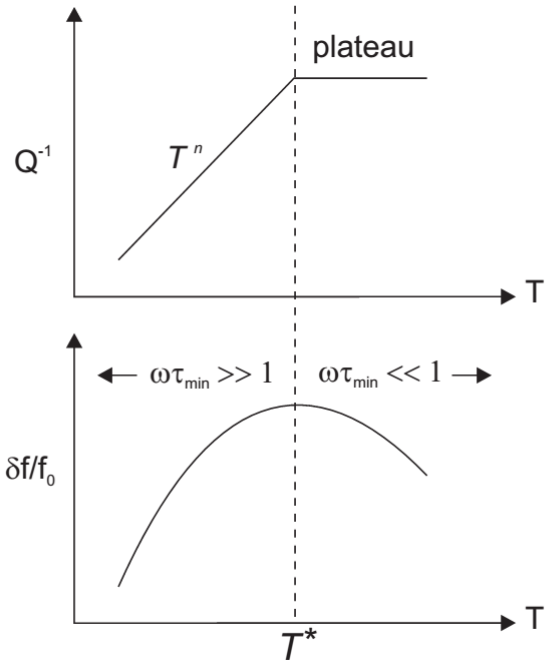

Figure 2.6: Generic predictions of the STM for the behaviour of dissipation and frequency shift as a function of temperature in an amorphous solid (Esquinazi 1998)

The frequency shift at temperatures below T^* is dominated by the resonant mechanism (the relaxation mechanism in this regime is negligible compared to the resonant process) and it increases logarithmically with slope C. Beyond T^* relaxation processes start to dominate the frequency shift and a logarithmic decrease with temperature is observed, the gradient of which is determined by the relaxation mechanism.

	$\frac{\delta f}{f}$		Q^{-1}	
Model	$T < T_{co}$	$T > T_{co}$	$T < T_{co}$	$T > T_{co}$
Single crystal	$\frac{C}{E}$	$\frac{C}{2k_B T}$	$\frac{b}{k_B T} e^{-\frac{2E}{k_B T}}$	dT^{-2}
Glass	$C \log\left(\frac{T}{T_0}\right)$	$-\frac{1}{2} C \log\left(\frac{T}{T_0}\right)$	aT^3	$\frac{1}{2\pi C}$
Phillips	$\propto \log\left(\frac{T}{T_0}\right)$	$\propto -\log\left(\frac{T}{T_0}\right)$	$\propto T$	Const.

Above table (Imboden and Mohanty 2013) shows the change in dissipation and frequency shift as described by various models(behavior for glass, single crystal, and Phillips model)

Chapter 3

Experimental Techniques

3.1 The Palladium Beam experiments

Pre-fabricated samples of palladium resonators were provide to study dissipation at low temperature.The SEM imaging (figure 3.1) was done to measure the dimensions of resonators to calculate the fundamental mode of resonate frequency .

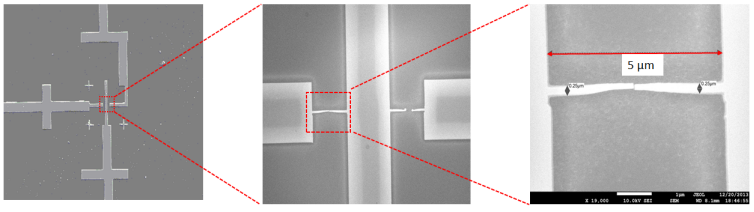

Figure 3.1: SEM micrograph of the measured palladium nano resonator.The studied sample is a 5μm long, 250 nm wide and 80 nm thick palladium resonator suspended above the silicon substrate.

The cryostat used for this investigation was Triton 200 by Oxford Instruments ^{3}He/^{4}He dilution refrigerator (figure3.5) with a base temperature of (10 $\pm$ 1) mK, equipped with a 2 axis 9/1 T magnet with cooling power of 200 μW at 100 mK. The measurements were carried out in transmission mode using R&S ZVB14 Vector Network Analyzer(figure 3.2. The sample was mounted on a PCB (figure 3.4 and figure 3.6) and placed inside a brass vacuum can (sealed with an indium O-ring) with electrical feed-through to the sample and resistance thermometers). The feed-throughs were filled with Stycast 2850FT . The magnetic field was applied perpendicular to the plane of the wafer in order to study the fundamental

in-the-plane flexural mode of the beam. Continuous wave magnetomotive scheme (section 3.3) were applied to study the motion of the beams.

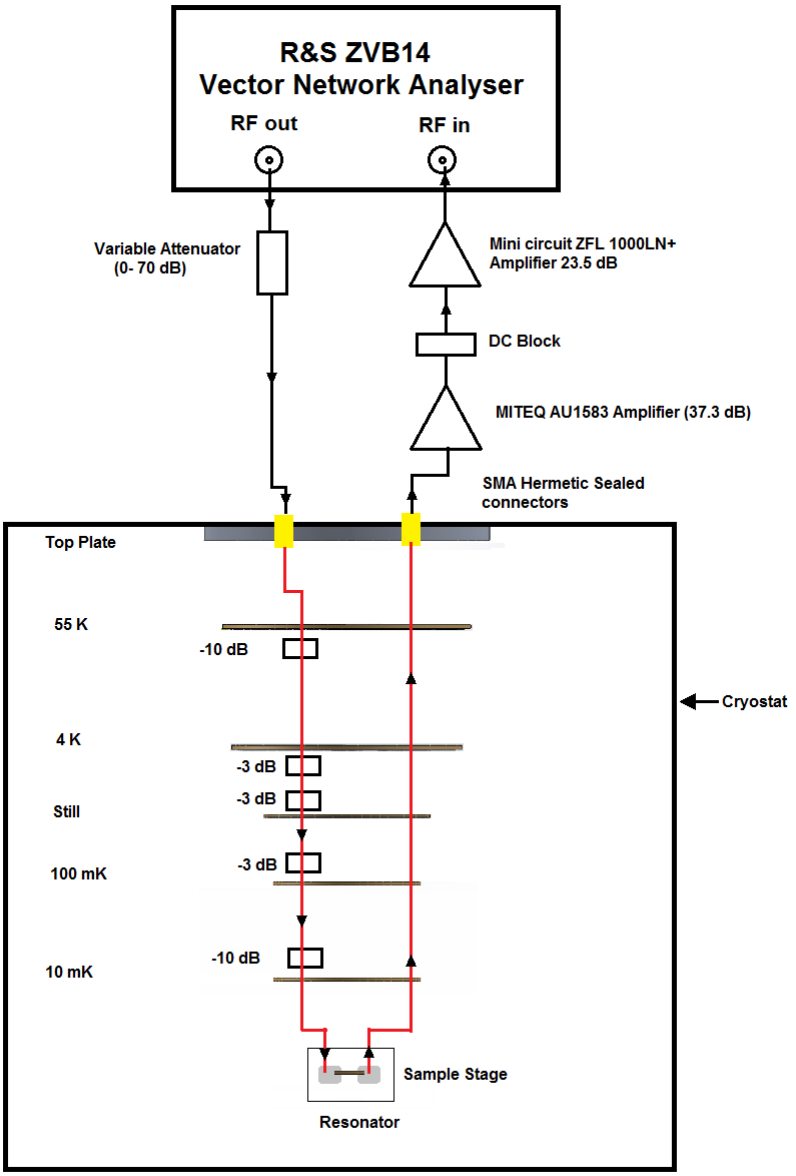

Figure 3.2: Schematic of the measurement setup and wiring inside the cryostat

3.2 Calibration of thermometer

A generic based thermometer was calibrated from 1.5 K down to 50 mK for using it to measure the temperature of the the palladium resonator mounted to sample stage in a brass

vacuum can. The RuO_2 resistance at the sample stage was calibrated against the one at the mixing chamber stage by letting the fridge stabilize for an hour at several temperatures between 1.5 K and 50 mK. The resistances of both chip resistors were then measured and assuming that both stages were at the same temperature, a calibration chart for the sample stage resistor was produced. The fig 3.3 shows the resistance in zero magnetic field as a function of $T^{-1/4}$ in a semi-log scale. The temperature variation of the resistance at lowest temperature is given by

$$R(T) \propto exp[(T_o/T)^p] \tag{3.1}$$

where p=1/4.(Watanabe, Morishita, and Ootuka 2001).

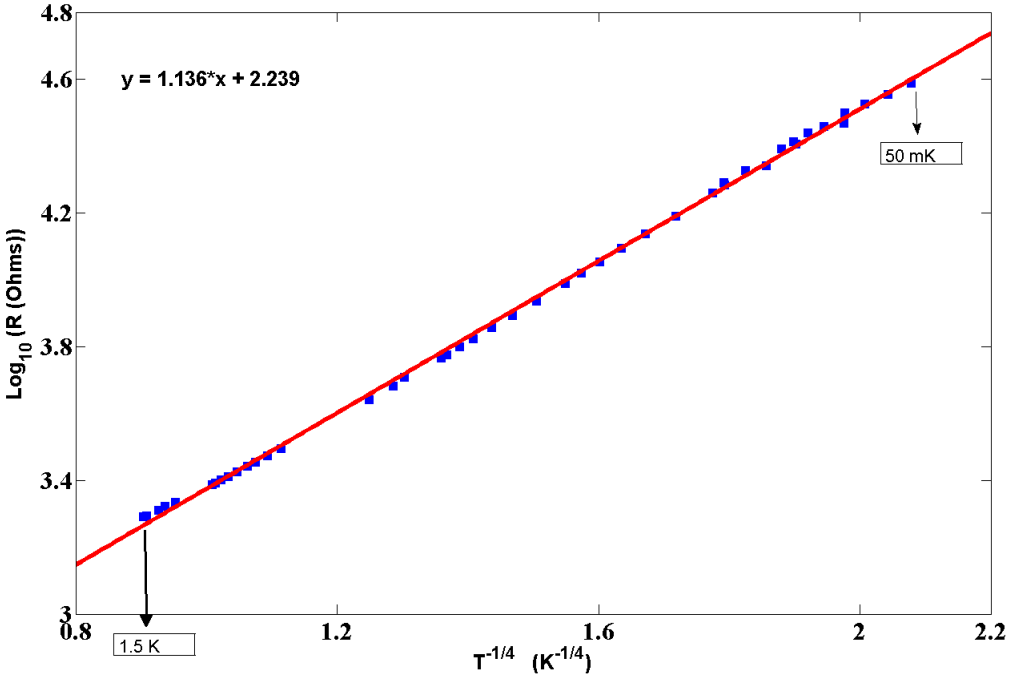

Figure 3.3: Calibration curve for a ruthenium Oxide based thermometer.The linear fit of resistance with $T^{-1/4}$ shows that the data obtained follows the equation 3.1

The resistance of RuO_2 based thermometer at low has been analyzed in terms of variable-range hopping(VRH) conduction(Shklovskii and Efros 1984).According to theory of VRH the value of p depends on the dimensionality d and the shape of the density of states around the fermi level.

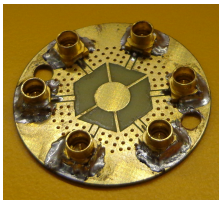

Figure 3.4: PCB for mounting sample with soldered surface mount super SMP connectors

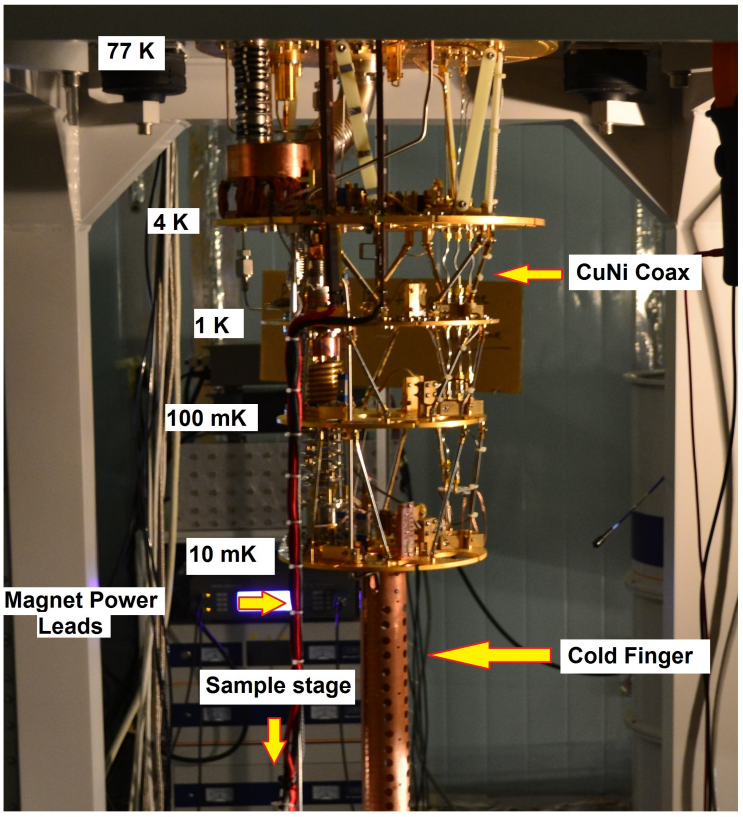

Figure 3.5: Photograph of Oxford instruments Triton 200 dilution refrigerator showing all cables and components from the 77 K flange to the sample stage after removing all the shields.

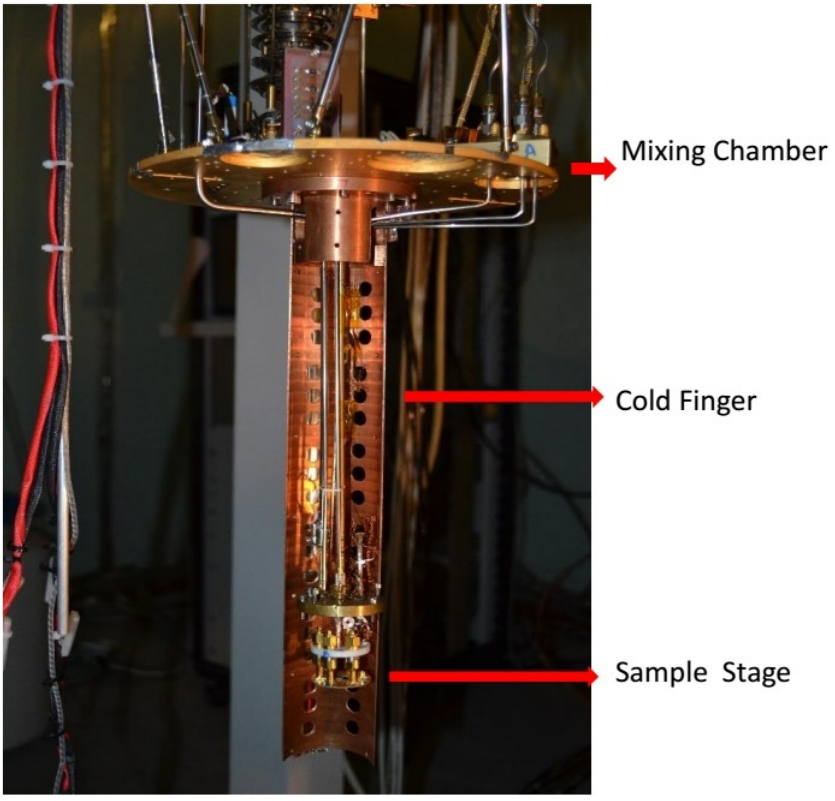

Figure 3.6: Copper cold finger thermally anchored from mixing chamber plate to vacuum can which was placed 370 mm below the plate in the center of 9 Tesla Magnet

3.3 Transduction Technique

Magnetomotive transduction,capacitive coupling to other electronic elements, piezoresistive actuation and optical detection are the few techniques to drive and detect the motion of nanomechanical resonators.

Magnetomotive technique is used in the experiment performed as it is simplest to implement.This technique was first developed by A. N. Cleland and M. L. Roukes (Cleland and Roukes 1999).The technique requires placing a conducting beam of length L in a uniform magnetic field B perpendicular to its longitudinal axis (figure 3.7). To drive the beam into motion a RF alternating current $I(t) = I_o e^{i\omega t}$ is applied where I_o and ω are the amplitude and frequency of oscillating current, so the beam experience an oscillating Lorentz force $F = LBI(t)$ of same frequency as applied signal perpendicular to both magnetic field and longitudinal axis of the beam.The motion of the beam can be described by the equation

$$\ddot{z} + \gamma\dot{z} + \omega_o^2 z = \frac{LBI(t)}{m} \tag{3.2}$$

where $z(t)$ is the displacement of the beam ,m its mass,$\gamma = \frac{\omega_o}{Q_o}$ is the damping coefficient.

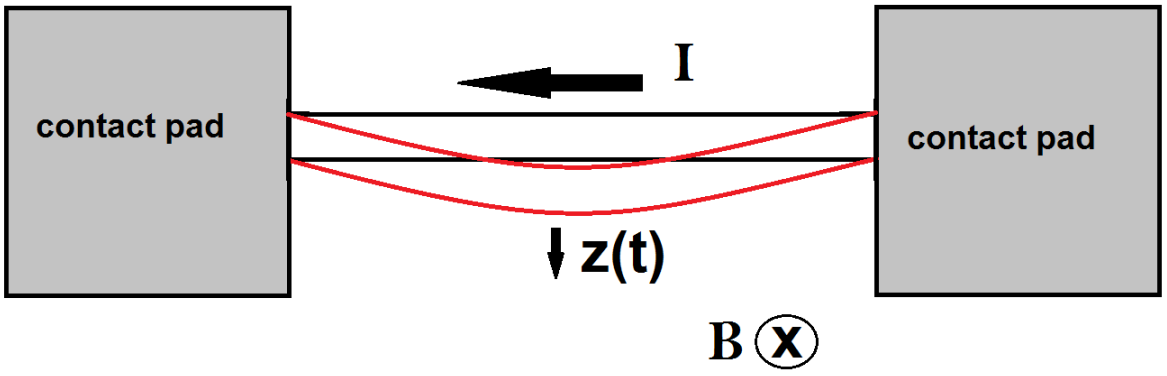

Figure 3.7: Schematic diagram of the magnetomotive drive and detection technique.

This motion of beam by Faradays Law,generates an electromotive force (EMF) $V_{EMF}(t) = \xi LBdz(t)/dt$ across it, which opposes the flow of current thereby increasing the impedance of the beam .The geometric constant ξ depends on the mode shape(0.83 for the fundamental mode for a doubly clamped beam).Substituting a solution of a form $z(t) = z_o e^{i\omega t}$ in equation 3.2,where z_o is the amplitude of displacement, the expression for beam displacement in terms of driving current becomes

$$z(t) = \frac{LBI(t)}{m(\omega_o^2 - \omega^2) + i\frac{m\omega\omega_o}{Q_o}} \tag{3.3}$$

Substituting the value of z(t) from equation 3.3 in equation 3.2 gives

$$V_{EMF} = i\omega\frac{\xi L^2 B^2 I(t)}{m(\omega_o^2 - \omega^2) + i\frac{m\omega\omega_o}{Q_o}} \tag{3.4}$$

On resonance the terms for induced EMF becomes

$$V_{EMF} = \frac{\xi L^2 B^2 Q_o I(t)}{m\omega_o} \tag{3.5}$$

Equivalent Circuit A nanomechnichal resonator is electrically equivalent to a parallel combination of an inductor L_m,a capacitor C_m and a resistor R_m while undergoing magnetomotive transduction as shown in fig 3.8.If the external impedence Z_{ext} is assumed to be

infinite,the voltage across ciruit is given by(Cleland and Roukes 1999)

$$V_{EMF} = i\omega \frac{\frac{I(t)}{C_m}}{(\omega_{LC}^2 - \omega^2) + \frac{i\omega}{R_m C_m}} \tag{3.6}$$

where $\omega_{LC} = \omega_o = 1/\sqrt{L_m C_m}$ is the resonant frequency of LCR circuit.

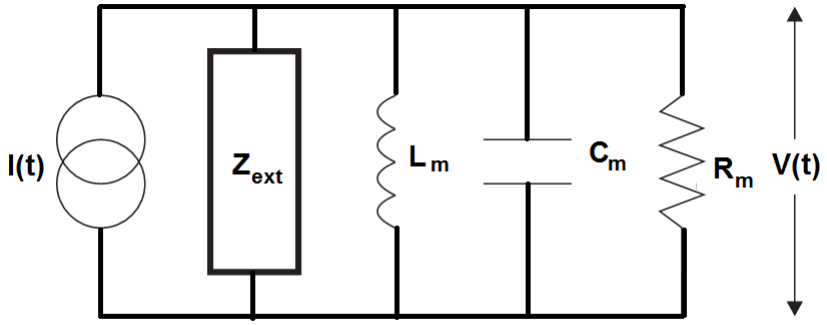

Figure 3.8: LCR representation of a mechanical resonator with a external impedance Z_{ext}, which represents the electrical resistance of the sample and measurement ciruit.

Equation 3.4 and 3.6 are analogous to each other where the model parameters in terms of mechanical properties of resonators are defined as

$$L_m = \frac{\xi L^2 B^2}{m\omega_o^2}, \quad C_m = \frac{m}{\xi L^2 B^2}, \quad R_m = \frac{\xi L^2 B^2}{m\omega_o^2} Q_o \tag{3.7}$$

If the external impedance is finite,the voltage across the whole circuit is(Cleland and Roukes 1999)

$$V_{EMF} = i\omega \frac{\frac{I(t)}{C_m}}{(\omega_o^2 + \frac{\omega\omega_o Z_e X_{ext}}{|Z_{ext}|^2}) - \omega^2 + i\omega(\frac{1}{Q_o} + \frac{Z_e R_{ext}}{|Z_{ext}|^2})} \tag{3.8}$$

where $R_{ext} = Re[Z_{ext}], X_{ext} = Im[Z_{ext}]$ and $Z_e = \sqrt{L_m/C_m}$. In this case the measured resonant frequency f_o and Q factor are not intrinsic,but related to circuit loaded values by

$$f_L = f_o \sqrt{1 + \frac{Z_e X_{ext}}{|Z_{ext}|^2}}; \quad Q_L^{-1} = Q_o^{-1} + \alpha B^2 \tag{3.9}$$

where $\alpha = \dfrac{\xi L^2}{m\omega_o}\dfrac{R_{ext}}{|Z_{ext}|^2}$. At any given temperature Q_o and α can be extracted by carrying out measurements as a function of magnetic field .

Although the magnetomotive technique is the easiest technique to implement for NEMS, it has some disadvantages. Firstly, it requires the use of magnetic fields generated by large superconducting coils, which need to be cooled down to cryogenic temperatures.Secondly,it is only possible to detect the odd flexural modes as the EMF voltages are canceled for the even modes.

3.4 Resonant Response Analysis

The transmission across resonator and the connecting RF cable is is measured using a Vector Network Analyzer.The measured response includes a background noise (fig 3.9) .

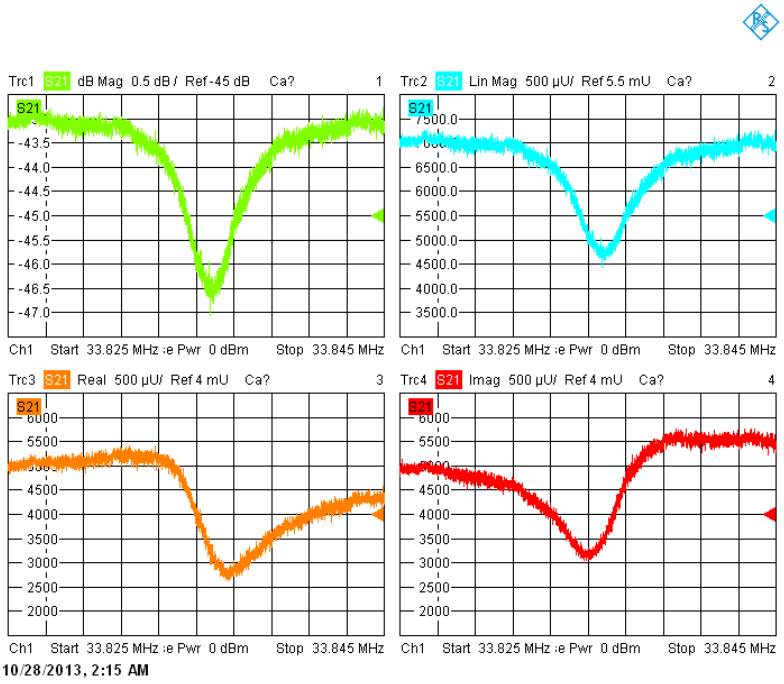

Figure 3.9: Figure shows the raw data obtained using a VNA.Plots are Log Amplitude,Amplitude, Inphase and quadrature response of the resonator including measurement setup

At small amplitudes a resonators motion can be modelled as a harmonic oscillator with a Lorentzian shaped resonant response. The method to fit the resonance curves obtained from the frequency domain measurements has been adapted from the method described in a thesis by I. Kozinsky For a Lorentzian superimposed on a background signal, the oscillator

response R has the following form(Kozinsky 2007):

$$R(\omega) = \frac{\frac{Ae^{i(\theta-\frac{3\pi}{2})}\omega_o^2}{Q}}{(\omega_o^2 - \omega^2) + \frac{i\omega\omega_o}{Q}} + B_0 + B_1(\omega - \omega_o) \tag{3.10}$$

which allows a full 8 parameter fit.($A_x, A_y, \omega_o, Q, B_{0x}, B_{0y}, B_{1x}, B_{1y}$) A is the resonant peak amplitude, ω_o the resonant frequency of the beam, Q its quality factor, the complex values B_0 and B_1 are the constant and frequency varying components of the background signal, respectively.The raw data are fitted to the above equation, the real and imaginary parts being fitted separately.The initial step is to fit the x and y components of the data to trace out a circle in the xy-plane (fig 3.10); this allows an estimate of the peak amplitude A which is given by the diameter of the circle. The phase factor $e^{i(\theta-\frac{3\pi}{2})}$ in the above equation accounts for the background phase, which shifts the circle from its zero background position (which is the origin). This phase is incorporated into the complex amplitude A . The next step is to fit the experimental values of $\frac{d\theta}{d\omega}$ which are background free and hence can be fitted to provide more accurate estimates of the resonant frequency and the Q-factor (fig 3.11).

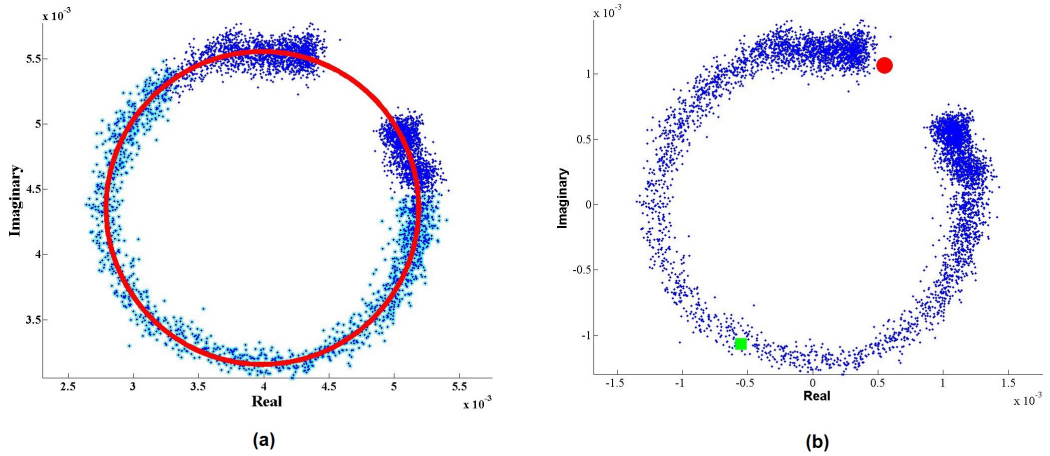

Figure 3.10: Figure a) A fitted circle to the imaginary vs real raw data b)The circle is translated such that center of circle coincides with origin,the amplitude is the diameter of circle and red point correspond to resonant frequency

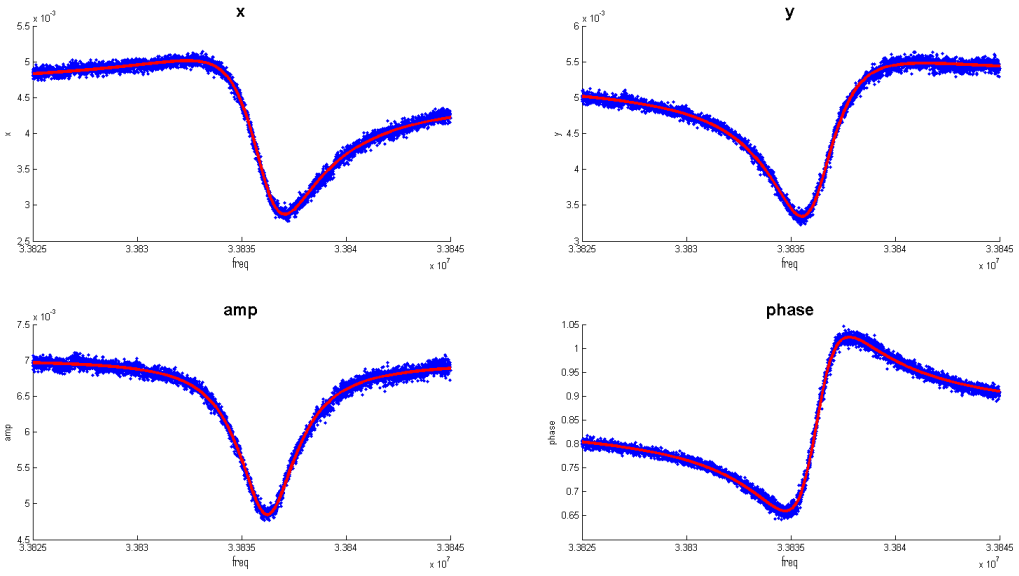

Figure 3.11: Real, imaginary ,amplitude and phase response of the typical measured response.The red line shows the fitted Lorentzian function after baseline correction

Chapter 4

Results

4.1 Device Frequency

The resonant frequency of nanomechanical resonators can depend significantly on the tension, T_o, in the structure. The tension arises from the difference in the thermal contraction between the substrate (silicon) and the metal (Pd) when the device is cooled down to low temperatures. The analytic expression for fundamental mode of a doubly-clamped beam as already discussed in section 2.2 is

$$f_{o1} = \frac{2\pi}{L^2}\sqrt{\frac{EI}{3\rho A}\left(1 + \frac{L^2 T_o}{4\pi^2 EI}\right)} \tag{4.1}$$

Using bulk values for the Youngs modulus (E = 124 GPa)(Vaz, Salvadori, and Cattani 2003) and density (ρ = 12093 kgm^{-3}) of Palladium,the expected frequencies without any stress is 33.53 MHz for the measured beam.The tension in beam can be estimated as $T_o = EA(\frac{\Delta L}{L})$ where $\frac{\Delta L}{L} = (\frac{\Delta L}{L})_{Pd} - (\frac{\Delta L}{L})_{Si}$ is the difference in the relative thermal contraction of Palladium and silicon.An estimate or the differential thermal contraction of palladium is 2.378 x 10^{-3}(Arblaster 2012) and 2.0 x 10^{-4} (Li et al. 2008)for silicon. These values were used to calculate an estimate for the tensile stress $\sigma = \frac{T_o}{A}$ in the beams when cooled from room temperature down to liquid helium temperatures, of about 386 MPa, leading to predicted resonant frequencies of 38.64 MHz .This is a crude estimate as the width of resonator does not remain uniform and varied from 180 μm at top to 250 μm at bottom.

4.2 Magnetic field dependence

Use of the magnetomotive transduction scheme results in a measured Q factor which is loaded by the external circuitry and the electrical resistance of the sample itself. Measurements of the magnetic field dependence of the resonator response were used to extract the resonators intrinsic Q-factor.Fig 4.2 shows plots of the dissipation as a function of B^2 for the sample at about 145 mK, which shows that the magnetic field can cause a significant change in the dissipation. As expected, the behaviour is found to be linear in B^2 and the gradient α allows Q_o^{-1} to be obtained by extrapolation to zero field.

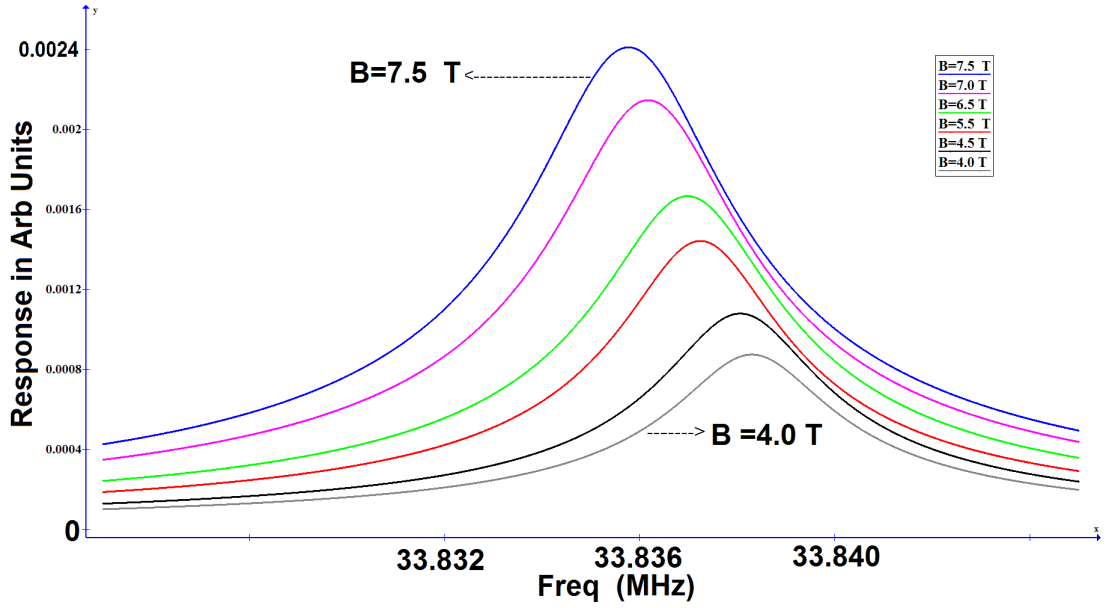

Figure 4.1: Response of a Pd beam at T = 145 mK at various Magnetic Field

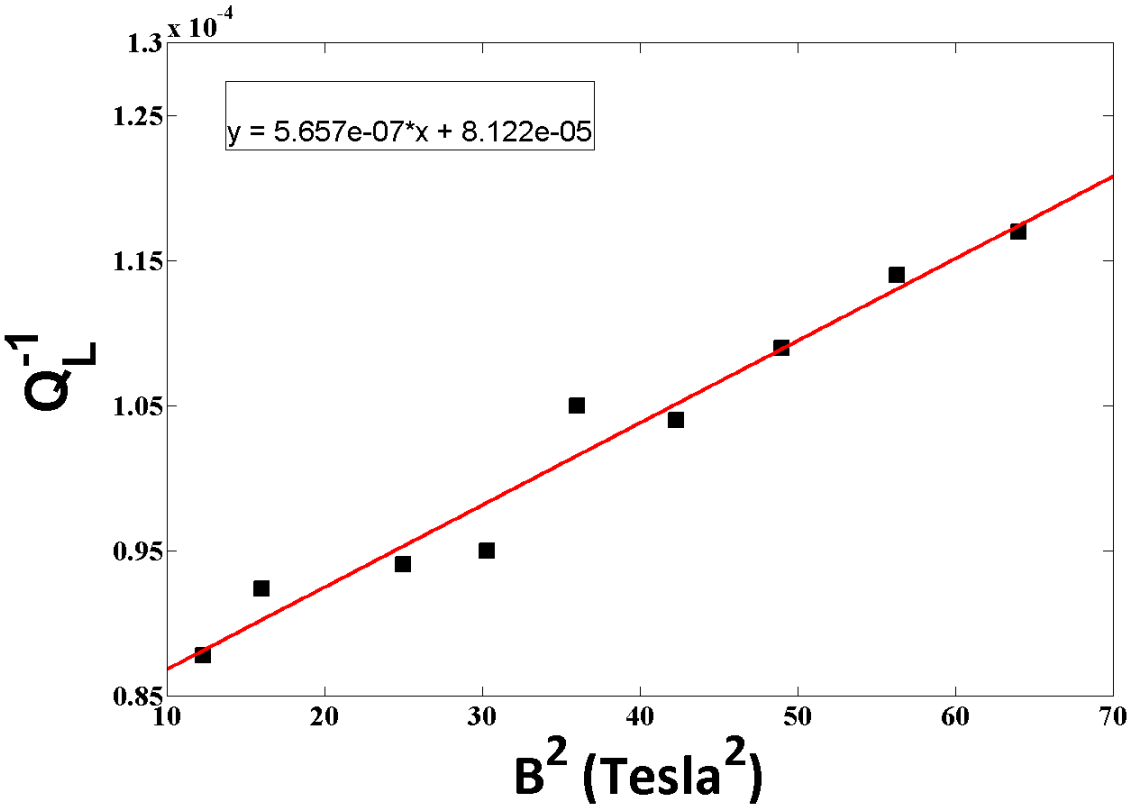

Figure 4.2: Plot of loaded dissipation as function of B^2.The red line is linear fit to data obtained.The slope gives value of α to be 5.67 x 10^{-7} and the intercept 8.122x 10^{-5} is the intrinsic dissipation of the resonator.

4.3 Temperature dependence

Measurements were carried out from about 1 K down to 145 mK at B=6 T as it provided an acceptable signal-to-noise ratio over the whole range of temperatures studie and the intrinsic quality factor and resonant frequency were extracted from the data.

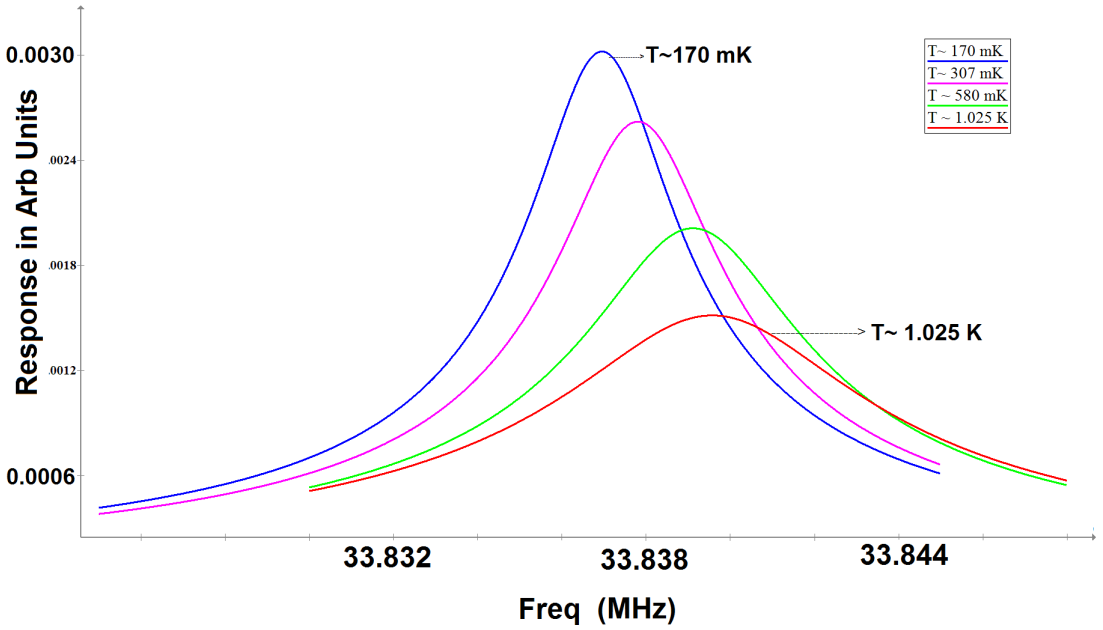

Figure 4.3: Response of a Pd beam at B=6 T for various Magnetic Field

4.3.1 Dissipation

Figure 4.4 shows the temperature dependence of the intrinsic dissipation.Two different regions of behavior can be identified. Below 200 mK the dissipation saturates, reaching what appears to be a plateau.In the region between 200 mk and 1 K, fits to the data show that the behavior of device is described by a power law T^n with n=0.466.

4.3.2 Resonant Frequency

The relative shift in the frequency of the resonators as a function of temperature is shown in Figure 4.5. There is an increase in frequency with temperature . The behavior here is well described by a logarithmic dependence $\frac{\Delta f}{f_o} = Clog\frac{T}{T^*}$.Using the slope and intercept of the fit from the data obtained,the value of C and T^* are estimated to be 115.6 x 10^{-6} and 1.134 K respectively.

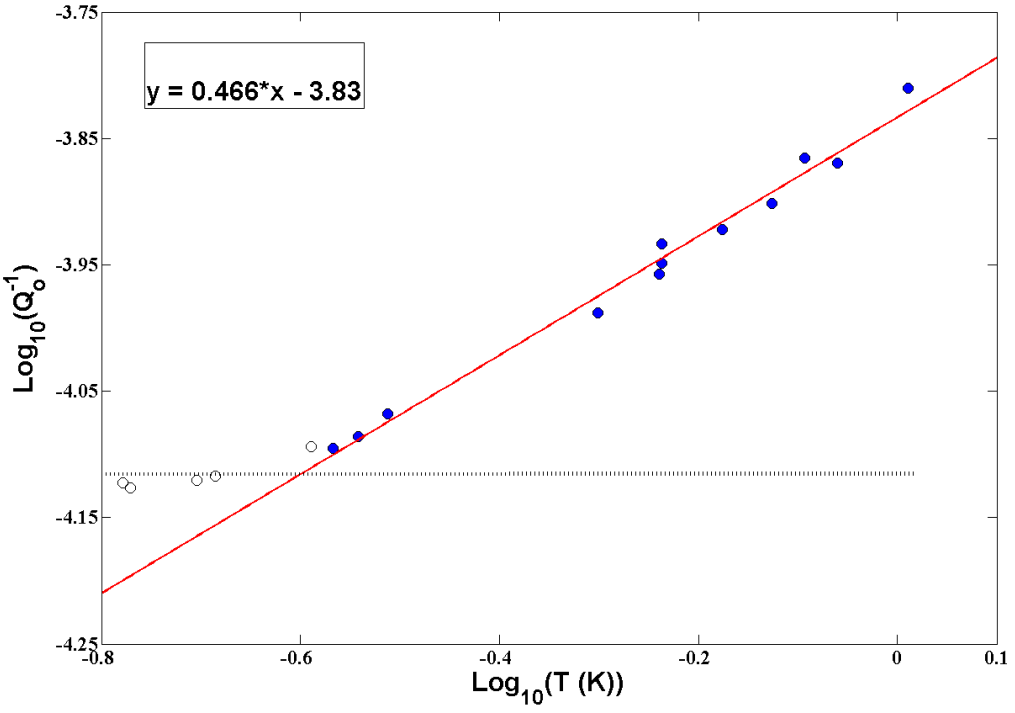

Figure 4.4: Intrinsic dissipation as a function of temperature on log-log scale

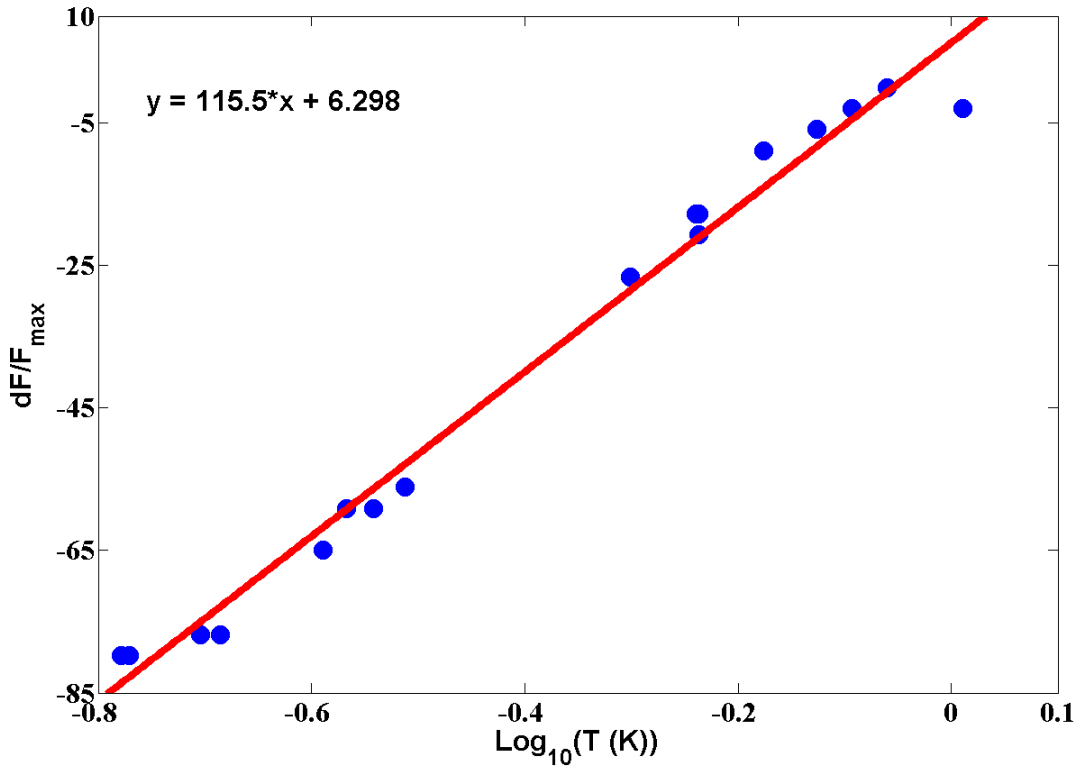

Figure 4.5: Relative shift in frequency as a function of temperature

4.4 Discussion

The strong variation seen in the dissipation at such low temperatures suggests that tunnelling TLS are the dominant source of dissipation.

Table 4.1 shows the estimated values of dissipation of the measured sample through different mechanism.The dissipation due to clamping plays negligible contribution to overall damping.The dissipation seen in the palladium fits the pattern predicted by the STM i.e. power law dependence $T^{0.47}$ at lower temperatures down to about 200 mK. However, the temperature dependence observed here is much lower than those predicted by the standard theories of acoustic damping in bulk solids.

Table 4.1: Estimated values of dissipation of the measured sample through different mechanism.The value of circuit damping was estimated by calculating difference between loaded and intrinsic dissipation at temperature=200 mK and Field =6 T.

Mechanism	**Estimated dissipation**
Clamping loss(2.20)	1×10^{-9}
Circuit Damping	2.6×10^{-5}
Quantum dissipation(at 200 mK)	8×10^{-5}

Table 4.2 shows the power law dependence for the other metallic resonators which have been already measured.(Venkatesan et al. 2009) (Hoehne et al. 2010) which are also much less than the predicted by the standard theories of acoustic damping in bulk solids. A plateau at higher temperature could not be seen due to lack of data above 1 K since the estimated value of T^* from frequency shift data is 1.134 K.The STM also predicts a frequency shift that increases logarithmically with temperature for $T \leq T^*$ due to the resonant interaction between the TLS and the acoustic excitation, with a gradient given by C .The logarithmic increase in the frequency shift that is seen below 1 K for the device agrees qualitatively with the STM.

Table 4.2: Summary of metallic resonators with $Q^{-1} \propto T^{\alpha}$ scaling law.

Material	**Value of α**
Palladium(measured)	0.47
Gold	0.5
Aluminium	1

4.5 Frequency Shift as a thermometer

A saturation was seen in the temperature dependence plot of dissipation.One possible reason may be the thermal decoupling between resonator and vacuum can.The thermometer is attached to the vacuum can, not the resonator,so it might give wrong estimation at such low temperature.One way to estimate the real temperature of resonator is by using frequency shift as it follows the logarithmic dependence even at low temperatures. Fig 4.6 show s temperature as a function of frequency shift on a semi-log scale,where red line shows the linear fit,confirming frequency shift follows the logarithmic dependence. So we can write

temperatures of resonator in terms of relative frequency shift as

$$T = antilog_{10}(8.0\frac{df}{F_{max}} - 76.1) \times 10^{-3} \tag{4.2}$$

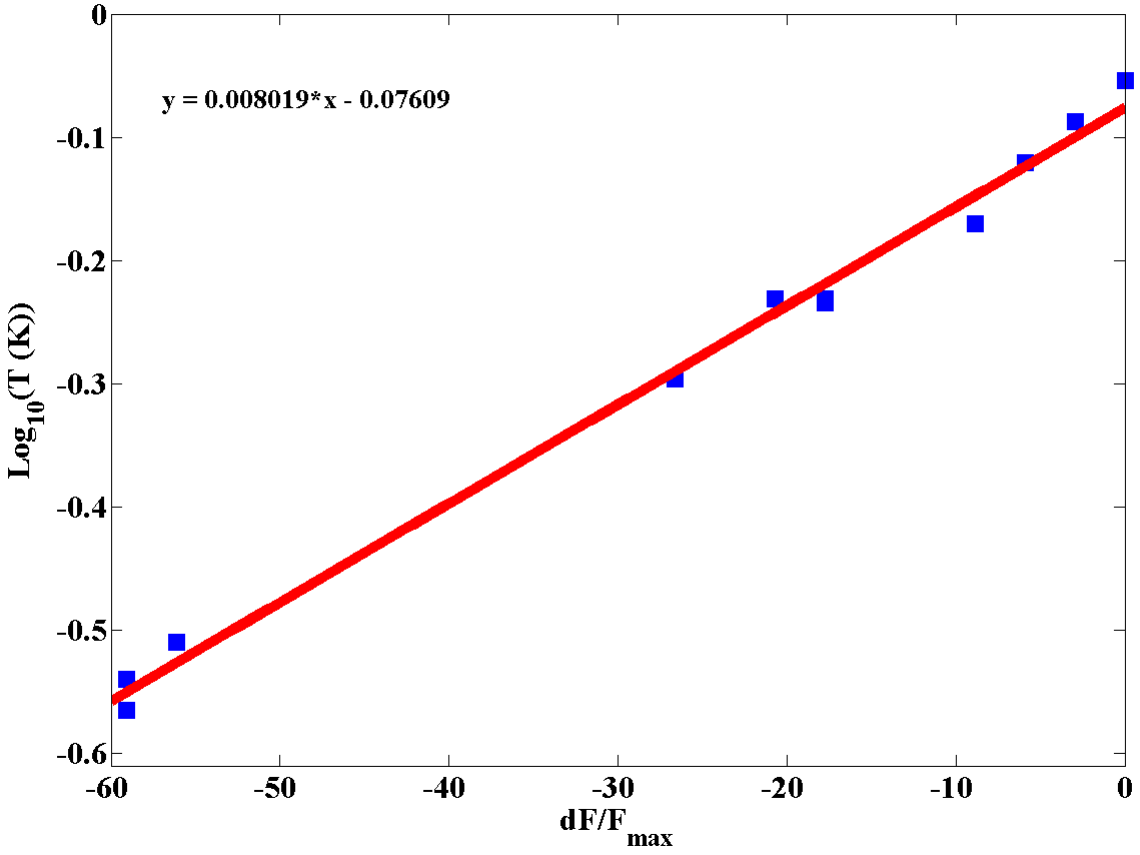

Figure 4.6: Temperature as a function of relative shift in frequency

Using equation 4.2 for the frequency shifts of data points below 200 mK, where dissipation appears to be saturating in figure 4.4 (white points) we can calculate new temperature and again plot the dissipation as a function of this new temperature and calculate new power law dependence which comes around to be $T^{0.41}$ (figure 4.7)

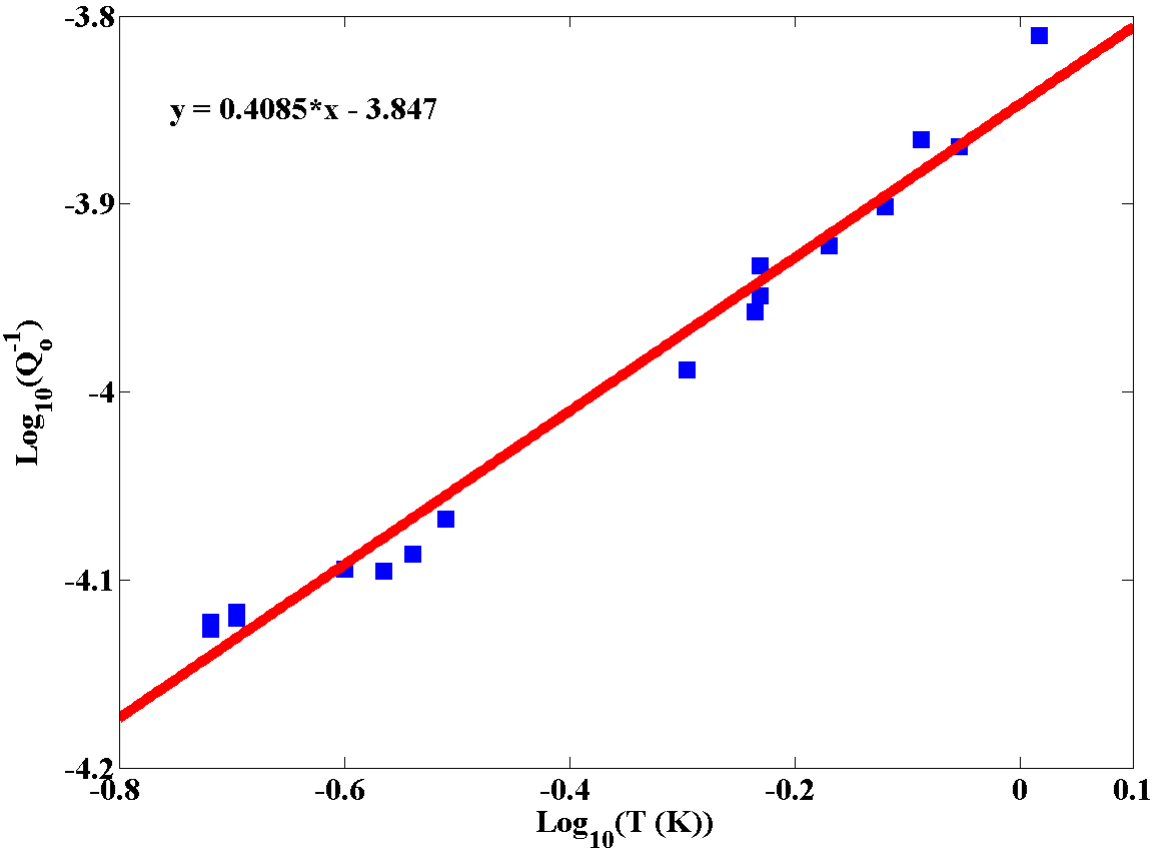

Figure 4.7: Modified Dissipation as function of temperature

4.6 Conclusion

In this thesis, the dissipation in palladium resonator at low temperatures have been studied. Their motion was actuated and detected using the magnetomotive transduction scheme. The samples were placed in a cryofree dilution refrigerators and all measurements were carried out at temperatures below 1 K using VNA. The resonance characteristics of the doubly-clamped palladium beams were measured as a function of magnetic field and temperature. By fitting the raw data to a Lorentzian function, we extracted the resonant frequency and Q-factor of the devices. The field dependence study allowed us to extrapolate to the B = 0 limit and infer the intrinsic quality factor of the resonators at any temperature. The dissipation in palladium nanomechanical resonators varies with temperature as $Q^{-1} \sim T^{0.47}$ between 200 mK and 1K and saturates below 200 mK. The resonant frequency of the beams increase logarithmically with temperature below 1 K.

The experiments described in this thesis provide initial results to understand the behavior of nanomechanical palladium resonators at low temperatures. However, additional measurements are needed to confirm the saturation below 200 mK and the quantitative value of temperature power dependence.Measurement above 1 K are also needed to get the full picture of dissipation behavior in the palladium resonator.The future work will also involve the study of electromechanical response of palladium beam resonator at low temperature in the presence of hydrogen gas as the palladium absorb hydrogen,so it alters the mass and tension of the resonator which can change the resonant frequency and quality factor.A vacuum can with hermetic DC and RF feedthroughs for cryogenic temperature has been prepared by another Masters student (Kumar 2014) .

Bibliography

[1] P. w. Anderson, B. I. Halperin, and c. M. Varma. "Anomalous low-temperature thermal properties of glasses and spin glasses". In: *Philosophical Magazine* 25.1 (Jan. 1972), pp. 1–9. ISSN: 0031-8086. DOI: 10.1080/14786437208229210. URL: http://dx.doi.org/10.1080/14786437208229210.

[2] John W. Arblaster. "Crystallographic Properties of Palladium". In: *Platinum Metals Review* 56.3 (July 2012), pp. 181–189. ISSN: 00321400. DOI: 10.1595/147106712X646113. URL: http://openurl.ingenta.com/content/xref?genre=article\&issn=0032-1400\&volume=56\&issue=3\&spage=181.

[3] A. Armour, M. Blencowe, and K. Schwab. "Entanglement and Decoherence of a Micromechanical Resonator via Coupling to a Cooper-Pair Box". In: *Physical Review Letters* 88.14 (Mar. 2002), p. 148301. ISSN: 0031-9007. DOI: 10.1103/PhysRevLett.88.148301. URL: http://link.aps.org/doi/10.1103/PhysRevLett.88.148301.

[4] Rustom B. Bhiladvala and Z. Jane Wang. "Effect of fluids on the Q factor and resonance frequency of oscillating micrometer and nanometer scale beams". In: *Physical Review E* 69.3 (Mar. 2004), p. 036307. ISSN: 1539-3755. DOI: 10.1103/PhysRevE.69.036307. URL: http://link.aps.org/doi/10.1103/PhysRevE.69.036307.

[5] A. Bokaian. "Natural frequencies of beams under tensile axial loads". In: *Journal of Sound and Vibration* 142.3 (Nov. 1990), pp. 481–498. ISSN: 0022460X. DOI: 10.1016/0022-460X(90)90663-K. URL: http://www.sciencedirect.com/science/article/pii/0022460X9090663K.

[6] Adrian Cho. "Physics. Researchers race to put the quantum into mechanics." In: *Science (New York, N.Y.)* 299.5603 (Jan. 2003), pp. 36–7. ISSN: 1095-9203. DOI: 10.1126/science.299.5603.36. URL: http://www.sciencemag.org/content/299/5603/36.short.

[7] A. N. Cleland and M. L. Roukes. “Noise processes in nanomechanical resonators”. In: *Journal of Applied Physics* 92.5 (Aug. 2002), p. 2758. ISSN: 00218979. DOI: 10.1063/1.1499745. URL: http://scitation.aip.org/content/aip/journal/jap/92/5/10.1063/1.1499745.

[8] A.N. Cleland and M.L. Roukes. “External control of dissipation in a nanometer-scale radiofrequency mechanical resonator”. In: *Sensors and Actuators A: Physical* 72.3 (Feb. 1999), pp. 256–261. ISSN: 09244247. DOI: 10.1016/S0924-4247(98)00222-2. URL: http://www.sciencedirect.com/science/article/pii/S0924424798002222.

[9] K. L. Ekinci and M. L. Roukes. “Nanoelectromechanical systems”. In: *Review of Scientific Instruments* 76.6 (May 2005), p. 061101. ISSN: 00346748. DOI: 10.1063/1.1927327. URL: http://scitation.aip.org/content/aip/journal/rsi/76/6/10.1063/1.1927327.

[10] Pablo Esquinazi. *Tunneling Systems in Amorphous and Crystalline Solids*. Springer-Verlag Berlin Heidelberg, 1998, p. 600. ISBN: 9783642083716.

[11] AP French. *Vibrations and Waves*. W . W . NORTON & COMPANY. INC. NEW YORK, 1971, pp. 62–68. DOI: 10.1007/SpringerReference_63.

[12] Xue Ming Henry Huang et al. “Nanoelectromechanical systems: Nanodevice motion at microwave frequencies.” In: *Nature* 421.6922 (Jan. 2003), p. 496. ISSN: 0028-0836. DOI: 10.1038/421496a. URL: http://dx.doi.org/10.1038/421496a.

[13] F. Hoehne et al. “Damping in high-frequency metallic nanomechanical resonators”. In: *Physical Review B* 81.18 (May 2010), p. 184112. ISSN: 1098-0121. DOI: 10.1103/PhysRevB.81.184112. URL: http://link.aps.org/doi/10.1103/PhysRevB.81.184112.

[14] S. Hunklinger and A. K. Raychaudhuri. *Progress in Low Temperature Physics, Volume 9 (Google eBook)*. Elsevier, 2011, p. 360. ISBN: 0080873049. URL: http://books.google.com/books?hl=en\&lr=\&id=OXpDBXTbly8C\&pgis=1.

[15] Matthias Imboden and Pritiraj Mohanty. “Dissipation in nanoelectromechanical systems”. In: *Physics Reports* (2013). URL: http://www.sciencedirect.com/science/article/pii/S0370157313003475.

[16] Robert G Knobel and Andrew N Cleland. “Nanometre-scale displacement sensing using a single electron transistor.” In: *Nature* 424.6946 (July 2003), pp. 291–3. ISSN: 1476-4687. DOI: 10.1038/nature01773. URL: http://dx.doi.org/10.1038/nature01773.

[17] Inna Kozinsky. “Nonlinear Nanoelectromechanical Systems”. PhD thesis. California Institute of Technology, 2007.

[18] Abhishek Kumar. “Hermetic RF feedthroughs for probing hydrogen absorbed palladium nanomechanical resonators at cryogenic temperatures”. MA thesis. Indian Institute of Science Education and Research Mohali, 2014.

[19] M D LaHaye et al. “Approaching the quantum limit of a nanomechanical resonator.” In: *Science (New York, N.Y.)* 304.5667 (Apr. 2004), pp. 74–7. ISSN: 1095-9203. DOI: 10.1126/science.1094419. URL: http://www.sciencemag.org/content/304/5667/74.abstract.

[20] T. F. Li et al. “High-frequency metallic nanomechanical resonators”. In: *Applied Physics Letters* 92.4 (2008), p. 043112. ISSN: 00036951. DOI: 10.1063/1.2838749. URL: http://link.aip.org/link/APPLAB/v92/i4/p043112/s1\&Agg=doi.

[21] Ron Lifshitz and M. Roukes. “Thermoelastic damping in micro- and nanomechanical systems”. In: *Physical Review B* 61.8 (Feb. 2000), pp. 5600–5609. ISSN: 0163-1829. DOI: 10.1103/PhysRevB.61.5600. URL: http://link.aps.org/doi/10.1103/PhysRevB.61.5600.

[22] HJ Pain. *THE PHYSICS OF VIBRATIONS*. Sixth Edit. John Wiley & Sons Ltd, 2005.

[23] W. A. Phillips. “Tunneling states in amorphous solids”. In: *Journal of Low Temperature Physics* 7.3-4 (May 1972), pp. 351–360. ISSN: 0022-2291. DOI: 10.1007/BF00660072. URL: http://link.springer.com/10.1007/BF00660072.

[24] W A Phillips. “Two-level states in glasses”. en. In: *Reports on Progress in Physics* 50.12 (Dec. 1987), pp. 1657–1708. ISSN: 0034-4885. DOI: 10.1088/0034-4885/50/12/003. URL: http://iopscience.iop.org/0034-4885/50/12/003.

[25] Douglas M. Photiadis and John A. Judge. “Attachment losses of high Q oscillators”. In: *Applied Physics Letters* 85.3 (July 2004), p. 482. ISSN: 00036951. DOI: 10.1063/1.1773928. URL: http://scitation.aip.org/content/aip/journal/apl/85/3/10.1063/1.1773928.

[26] D Rugar et al. “Single spin detection by magnetic resonance force microscopy.” In: *Nature* 430.6997 (July 2004), pp. 329–32. ISSN: 1476-4687. DOI: 10.1038/nature02658. URL: http://dx.doi.org/10.1038/nature02658.

[27] Vera Sazonova et al. “A tunable carbon nanotube electromechanical oscillator.” In: *Nature* 431.7006 (Sept. 2004), pp. 284–7. ISSN: 1476-4687. DOI: 10.1038/nature02905. URL: http://dx.doi.org/10.1038/nature02905.

[28] Boris I. Shklovskii and Alex L. Efros. *Electronic Properties of Doped Semiconductors*. Vol. 45. Springer Series in Solid-State Sciences. Berlin, Heidelberg: Springer Berlin Heidelberg, 1984. ISBN: 978-3-662-02405-8. DOI: 10.1007/978-3-662-02403-4. URL: http://link.springer.com/10.1007/978-3-662-02403-4.

[29] V.A.Sazonova. “A TUNABLE CARBON NANOTUBE RESONATOR”. PhD thesis. Cornell University, 2006.

[30] A.R Vaz, M.C Salvadori, and M. Cattani. *Young Modulus Measurement of Nanostructured Palladium Thin Films*. 2003. URL: http://www.nsti.org/procs/Nanotech2003v3/4/T55.01.

[31] A. Venkatesan et al. “Dissipation in a Gold Nanomechanical Resonator at Low Temperatures”. In: *Journal of Low Temperature Physics* 158.3-4 (Sept. 2009), pp. 685–691. ISSN: 0022-2291. DOI: 10.1007/s10909-009-9951-6. URL: http://link.springer.com/10.1007/s10909-009-9951-6.

[32] Michio Watanabe, Masashi Morishita, and Youiti Ootuka. “Magnetoresistance of RuO2-based resistance thermometers below 0.3 K”. In: *Cryogenics* 41.3 (Mar. 2001), pp. 143–148. ISSN: 00112275. DOI: 10.1016/S0011-2275(01)00066-2. URL: http://www.sciencedirect.com/science/article/pii/S0011227501000662.

[33] Y T Yang et al. “Zeptogram-scale nanomechanical mass sensing.” In: *Nano letters* 6.4 (Apr. 2006), pp. 583–6. ISSN: 1530-6984. DOI: 10.1021/nl052134m. URL: http://dx.doi.org/10.1021/nl052134m.